AAS 09-424

AN ASSESSMENT OF MULTIPLE SATELLITE-AIDED CAPTURE AT JUPITER

Alfred E. Lynam[*], Kevin W. Kloster[†], and James M. Longuski[‡]

Satellite-aided capture is a mission design concept used to reduce the delta-v required to capture into a planetary orbit. The technique employs close flybys of a massive moon to reduce the energy of the planet-centered orbit. A sequence of close flybys of two or more of the Galilean moons of Jupiter may further decrease the delta-v cost of Jupiter orbit insertion. A Ganymede-Io sequence saves 207 m/s of delta-v over a single Io flyby. These sequences have the potential to benefit both NASA's Jupiter Europa orbiter mission and ESA's Jupiter Ganymede orbiter mission.

INTRODUCTION

The propellant required to capture into orbit at another planet is costly to carry across the Solar System. Any reduction in capture ΔV can result in a significant decrease in the mass and cost of the spacecraft. One method of reducing the ΔV required for capture into orbit at another planet is to use gravity-assist maneuvers at the moons of the planet. This satellite-aided capture technique was first proposed for the Jupiter system by Longman[1] and Longman and Schneider.[2] They showed that gravity-assist flybys of the Galilean moons could help capture a spacecraft into orbit about Jupiter. The analysis demonstrated the effect of one- and two-moon encounters on the orbital energy of the incoming Jupiter-centered, hyperbolic orbit. Cline[3] determined the minimum ΔV required for a capture sequence involving a single flyby of Ganymede and a Jupiter orbit insertion (JOI) maneuver.

The effects of various flyby parameters on the efficiency of satellite-aided capture are investigated by Nock and Uphoff.[4] The parameters they vary are: perijove radius after flyby, flyby altitude, declination of the incoming satellite-centered hyperbola, and the distribution of ΔV between powered satellite flybys and the JOI maneuver. In addition, they determine the phasing and transfer orbit parameters necessary to accomplish double-satellite-aided capture. Malcolm and McInnes[5] formulate a solution to the satellite-aided capture problem using a vectorial flyby targeting technique. Yam[6] presents an analytical technique for targeting a planet-centered V_∞ vector to the position vector of a moon which determines the phase angle between the incoming Jupiter-centered asymptote and the flyby encounter.

The Galileo mission to Jupiter was the first mission to implement satellite-aided capture. In 1995, the Galileo orbiter executed a medium-altitude flyby of Io to decrease the JOI ΔV requirements by 175 m/s to 644 m/s[7] (its targeted flyby altitude was 1000 km, but its actual flyby altitude was 892 km). The Europa Orbiter Mission[8–10] and the Jupiter Icy Moons Orbiter[11] had prepared single satellite-aided capture trajectories using Ganymede and Callisto, respectively.

We extend the gravity assist technique to include close flybys of multiple Galilean moons during Jupiter capture. The entire solution space of efficient, multiple-satellite-aided capture trajectories at Jupiter is systematically explored by categorizing capture sequences into four different types based on flyby geometry and timing: double-satellite-aided capture, Laplacian[12–15] triple- satellite-aided capture (Ganymede, Europa, and Io), Callistan triple-satellite-aided capture (Callisto and two others), and quadruple-satellite-aided capture.

[*]Graduate Student, School of Aeronautics & Astronautics, Purdue University, 701 W. Stadium Ave. West Lafayette, IN 47907-2045.
[†]Graduate Student, AIAA Student Member, School of Aeronautics & Astronautics, Purdue University, 701 W. Stadium Ave. West Lafayette, IN 47907-2045.
[‡]Professor, AAS Member, AIAA Associate Fellow, School of Aeronautics & Astronautics, Purdue University, 701 W. Stadium Ave. West Lafayette, IN 47907-2045.

ASSUMPTIONS AND METHODOLOGY

We employ several simplifying assumptions to design multiple-satellite-aided capture trajectories. Because the Galilean moons have low orbital eccentricities and inclinations, they are assumed to be in circular, coplanar orbits about Jupiter. Trajectory sequences with multiple flybys are designed in an ephemeris-free, patched-conic model where each moon flyby represents a discrete event in the Jupiter-centered trajectory. For periodic flyby sequences, we give a repeat-time interval based on the synodic period of the desired moons. This model also assumes that the incoming interplanetary trajectory can be adjusted to align with the first flyby. We ignore all retrograde capture strategies because all of the Galilean moons are in direct orbits about Jupiter.

These assumptions enable the multiple-satellite-aided capture problem to be studied in isolation from the timing and interplanetary trajectory problems. The patched-conic model is useful in this application because the entire capture sequence occurs quickly, which limits the effects of perturbing accelerations.

Several of the capture trajectories designed using the patched-conic model are integrated in a full-ephemeris model (AGI's STK/Astrogator[16]) to ensure that the trajectories physically exist. In this model, the full gravity fields (including spherical harmonics) of the Sun, Jupiter, Io, Europa, Ganymede, and Callisto are applied to a spacecraft placed along a Jupiter-approach asymptote. Solar radiation pressure and general relativity perturbations are also applied to maximize the fidelity of the solutions. The starting time and angular parameters of the approach asymptote are varied to target the B-plane parameters of the inbound moon flybys, while the magnitude and direction of the JOI maneuver are used to target the outbound flybys and capture orbit period.

Using the STK model, we determine whether flyby sequences align with near-Hohmann interplanetary trajectories by finding the right ascension (RA) of their approach asymptote and determining how close it is to the RA for a Hohmann trajectory. If it is within 10 degrees of the Hohmann RA, its interplantary trajectory will at least approach Earth's orbital radius. Furthermore, we ignore the phasing of the Earth.

In our analysis, we set aside the issue of how to navigate such captures. First we must examine the potential benefits in a deterministic model and assess the physical realizability of these trajectories. Only after resolving deterministic feasibility, can we begin to answer the question of whether these benefits can be realistically achieved with current navigation capabilities or with capabilities that may become available in the near future (e.g. via autonomous navigation). We do, however, use the delta-Delta-v method[17] to perform a sensitivity analysis for flyby errors. For example, if the first flyby of a sequence has a small error, this error will propagate geometrically to a medium error in the second flyby, and to a much larger error in the third or fourth flybys. This analysis roughly assesses the difficulties of navigating these flyby sequences without actually solving them.

PATCHED-CONIC METHOD OF INTERMOON TRANSFERS

The patched-conic method has been applied extensively as a first-order approximation of the three-body problem.[1–6,18] The input parameters for a gravity-assist flyby are the pre-flyby semi-major axis (a_{in}) orbital energy ($\mathcal{E}_{\text{in}}$), or V_∞; and the eccentricity(e_{in}) or perijove ($R_{\text{p,in}}$) of the Jupiter-centered orbit. The gravity-assist algorithm provides the moon-centered, hyperbolic-excess velocity ($V_{\infty,\text{moon}}$) and the post-flyby Jovicentric semi-major axis (a_{out}) and eccentricity (e_{out}). These outputs are used as inputs into the same algorithm for the next flyby in the sequence until the last flyby in the sequence is completed. The process provides the semi-major axes and eccentricities of every transfer orbit in the flyby sequence.

True Anomaly and Time of Flight

The patched-conic algorithm provides sufficient information (i.e. approximate values for $a_{\text{sc,out}}$ and $e_{\text{sc,out}}$) to determine the true anomaly relations and the time of flight for the entire trajectory sequence. First, we compute the difference in the true anomalies between the incoming Jupiter arrival asymptote and the first moon flyby using the method developed by Yam.[6]

$$\Delta f = 360^\circ - f_{\text{moon}} + f_\infty \tag{1}$$

where

$$f_{\text{moon}} = -\cos^{-1}\left[\frac{-a_{\text{moon}} + a_{\text{sc,in}}(1-(e_{\text{sc,in}})^2)}{a_{\text{moon}}e_{\text{sc,in}}}\right] \tag{2}$$

$$f_{\infty} = -\cos^{-1}\left[\frac{1}{e_{\text{sc,in}}}\right] \tag{3}$$

where f_{moon} is the true anomaly of the spacecraft's orbit when it reaches the desired moon, f_{∞} is the true anomaly of the spacecraft's orbit along the approach asymptote, and Δf is the difference in the true anomalies between the two positions. The time of flight from the asymptote to the moon is infinite in the conic model, so time-of-flight computations are not meaningful.

Next, we determine the true anomalies and time of flight for the transfer leg from the first flyby to a second flyby. The equations used are similar to those given by Nock and Uphoff[4]

$$\Delta f_{1,2} = f_{\text{moon},1} - f_{\text{moon},2} \tag{4}$$

where

$$f_{\text{moon}} = -\cos^{-1}\left[(-a_{\text{moon}} + a_{\text{sc,out}}(1-(e_{\text{sc,out}})^2))/(a_{\text{moon}}e_{\text{sc,out}})\right] \tag{5}$$

where $f_{\text{moon},1}$ is the true anomaly of the spacecraft at the first moon, $f_{\text{moon},2}$ is the true anomaly of the spacecraft at the second moon, and $\Delta f_{1,2}$ is the difference in the true anomalies of the encounters. If the spacecraft is still in a hyperbolic orbit during this transfer leg, the hyperbolic anomalies of both of the encounters ($H_{\text{moon},1}$ and $H_{\text{moon},2}$) can be found and the time of flight ($T_{1,2}$) computed from:

$$T_{1,2} = \sqrt{-(a_{\text{sc,out}})^3/\mu_{\text{J}}}\left[(e_{\text{sc,out}}\sinh H_{\text{moon},2} - H_{\text{moon},2}) - (e_{\text{sc,out}}\sinh H_{\text{moon},1} - H_{\text{moon},1})\right] \tag{6}$$

where

$$H_{\text{moon}} = -\cosh^{-1}\left[(a_{\text{sc,out}} - a_{\text{moon}}/(a_{\text{sc,out}}e_{\text{sc,out}})\right] \tag{7}$$

For low incoming V_{∞} values, such as those given by low-thrust trajectories, it is possible that the spacecraft may have captured into a tenuous, long-period elliptical orbit after the first flyby. If that is the case, we modify the method to calculate the eccentric anomalies ($E_{\text{moon},1}$ and $E_{\text{moon},2}$) of the spacecraft at the two encounters and solve Kepler's equation for time of flight ($T_{1,2}$)

$$T_{1,2} = \sqrt{(a_{\text{sc,out}})^3/\mu_{\text{J}}}\left[(E_{\text{moon},2} - e_{\text{sc,out}}\sin E_{\text{moon},2}) - (E_{\text{moon},1} - e_{\text{sc,out}}\sin E_{\text{moon},1})\right] \tag{8}$$

where

$$E_{\text{moon}} = -\cos^{-1}\left[(a_{\text{sc,out}} - a_{\text{moon}})/(a_{\text{sc,out}}e_{\text{sc,out}})\right] \tag{9}$$

After the final flyby of the incoming leg, the spacecraft performs a JOI maneuver at its perijove. The difference between the true anomalies and the time of flight between the final flyby and the perijove are determined by Equations (5) – (8) with the final hyperbolic/eccentric, and true anomalies defined to be zero. The effect of the JOI delta-v (ΔV_{JOI}) on the spacecraft's orbit is determined from the perijove and orbital energy of the orbit before the maneuver:

$$V_{\text{p,in}} = \sqrt{2\left(\mathcal{E}_{\text{p,in}} + \mu_{\text{J}}/R_{\text{p,in}}\right)} \tag{10}$$

where $V_{\text{p,in}}$ is the velocity at perijove before the maneuver, $\mathcal{E}_{\text{p,in}}$ is the orbital energy before the maneuver, and $R_{\text{p,in}}$ is the radius of the perijove of the orbit:

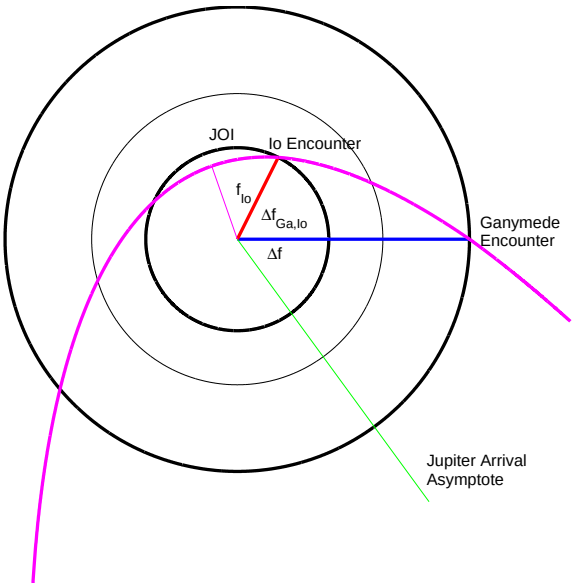

Figure 1 Graphical representation of the angle between the asymptote and the Ganymede encounter(Δf), angle between Ganymede and Io encounters ($\Delta f_{\mathbf{Ga,Io}}$), and the angle between the Io encounter and JOI at perijove ($f_{\mathbf{Io}}$).

$$V_{\text{p,out}} = V_{\text{p,in}} - \Delta V_{\text{JOI}} \tag{11}$$

$$\mathcal{E}_{\text{p,out}} = (V_{\text{p,out}})^2/2 - \mu_{\text{J}}/R_{\text{p,out}} \tag{12}$$

where $V_{\text{p,out}}$ is the velocity at perijove after the maneuver and $\mathcal{E}_{\text{p,out}}$ is the orbital energy after the maneuver.

If there are any encounters after the JOI maneuver, the phase angles and times of flight can be computed by modifying the above methods. Outbound encounters cause the sign of the hyperbolic, eccentric, and true anomalies to change from negative to positive. Another change is that the spacecraft travels from the inner moons to the outer moons rather than vice versa.

HIGH-FIDELITY TRAJECTORY INTEGRATION USING STK

We validate the existence of multiple-satellite-aided capture trajectories discovered using the patched-conic model via numerical integration. Sample trajectories from the patched-conic model are input into AGI's STK 8.1.3 software[16] to find full-ephermeris, high-fidelity trajectories. We design these trajectories such that they begin several days before the modeled spacecraft reaches Callisto's orbit.

With this strategy, we develop algorithms to discover individual capture sequences and then find equivalent sequences every synodic period (for double- and Laplacian triple-satellite-aided-capture sequences) or aperiodically (for Callistan triple-satellite-aided capture and quadruple-satellite-aided capture). After searching through enough dates, any particular type of satellite-aided capture sequence will indubitably align with an interplanetary trajectory. We perform a direct analysis of the interplanetary flyby windows for three different types of double flyby sequences. Since triple- and quadruple-satellite-aided capture sequences occur much less frequently than double-satellite-aided capture sequences, so it is more difficult to predict when they align with interplanetary trajectories. When a satellite-aided capture trajectory does happens to align with an available interplanetary trajectory from Earth, the trajectory could be integrated backwards to Earth using STK's backwards-propagation function.

Spacecraft and Software Parameters

A propagator for the trajectories was defined using STK's best gravity fields for the Sun, Jupiter, Ganymede,[19] Callisto,[20] Io,[21] and Europa.[22] The higher-order, spherical-harmonic expansion terms implemented for each of the gravity fields are listed in Table 1. Additionally, solar radiation pressure and general relativity effects were included in the propagator. The exposed area for solar radiation pressure was estimated to be 12.42 m^2 from the spacecraft model in NASA's JEO mission report.[23] The JOI manuever was modeled as a finite burn beginning at perijove with an Isp of 323 seconds and a thrust of 890 N.[23]

Table 1. STK Gravity Fields

Gravity Fields	Sun	Jupiter	Ganymede	Callisto	Io	Europa
GM (km^3/s^2)	1.327122 x 10^{11}	1.26686535 x 10^8	9886.6	7169.292	5960	3202.72
J2 (x 10^{-6})	—	-14696.43	-127.27	-32.7	-1845.9	-435.5
C22 (x 10^{-6})	—	—	38.18	10.2	553.7	131.0
S22 (x 10^{-6})	—	—	—	-1.1	—	-11.9
J3 (x 10^{-6})	—	0.64	—	—	—	—
J4 (x 10^{-6})	—	587.14	—	—	—	—
J5 (x 10^{-6})	—	0	—	—	—	—
J6 (x 10^{-6})	—	-34.25	—	—	—	—

The high-fidelity of the propagator is necessary because of the numerical sensitivity of the multiple-satellite-aided capture sequences. For a Ganymede-Io-JOI-Europa-Callisto four-flyby capture sequence, the spacecraft was optimally inserted into an 87-day orbit with only a point-mass gravity model for all six bodies. However, the high-fidelity model with oblateness, Solar radiation pressure, and general relativity converged on a 168-day orbit as the optimal sequence. These differences are not sufficient to preclude the possibility of a sequence occurring at a given time, but they do substantially affect the results of certain sequences, especially Callistan triple-satellite-aided capture sequences and quadruple-satellite-aided capture sequences.

STK Targeting Algorithm

STK employs a differential-corrector targeting algorithm that varies a user-defined set of control variables to converge on another user-defined set of target variables (within a specified tolerance). The targeter first propagates the nominal sequence and determines the initial values of the target variables. The targeter then perturbs each control variable and uses finite differencing to determine a matrix of partial derivatives. The matrix is used to correct the control variables in the nominal trajectory and re-propagate the trajectory such that the target variables are closer to their desired values. This process is repeated until the target variables are equal to their desired values (within an acceptable tolerance).

Although each type of sequence requires a unique targeting algorithm, most of the control and target variables remain the same for all sequences. The potential control parameters contained in the arrival asymptote are initial time (Epoch), declination (Dec), right ascension of the approach asymptote (RA), the velocity azimuth at perijove ($V_{\text{azimuth,p}}$), target perijove (R_{p}), C_3 energy, and true anomaly. Various combinations of these control variables were tested with STK's targeting algorithm and we determined that target perijove, C3 energy, and true anomaly are ineffective as control parameters in the targeting sequence, so they are fixed at their nominal values. However, the nominal values of these three variables can be manually modified to change the trajectory solutions. The JOI manuever can also be used as a control with either one (thrusting directly against the velocity vector) or three (a vector maneuver) control variables. Thus, the total number of potential control parameters is seven: Epoch, Dec, RA, $V_{\text{azimuth,p}}$, and the three $\mathbf{\Delta V}_{\text{JOI}}$ manuever components.

The target parameters are the B-plane parameters of each of the moons and the C_3 energy of the final orbit. An optimal flyby occurs at a B-plane angle of 0 degrees for inbound encounters and a B-plane angle of 180 degrees for an outbound encounter. Thus, the target B-plane parameters are 0 for $B \cdot R$, a positive value for $B \cdot T$ that corresponds with the desired flyby altitude for inbound flybys and a negative value for $B \cdot T$ that

corresponds with the desired flyby altitude for outbound flybys. Hence, the number of target parameters is one plus two times the number of gravity-assist flybys.

On some flyby sequences, the available control parameters are insufficient to converge all of the target parameters. In those cases, either the target perijove can be manually varied, the targeted capture orbit period can be freed, or the B-plane parameters on one of the flybys can be allowed to become suboptimal. Manually changing parameters increases the amount of time required to converge trajectories because the sequence has to be re-converged every time the parameters are manually varied. Also, the suboptimal flybys of some moons cause the entire capture sequence to become less ΔV-efficient.

NAVIGATION AND OPERATIONS REQUIREMENTS

All of the trajectories described in this paper so far are deterministic trajectories. If the acceleration models, ephemerides, and spacecraft position and velocity were known perfectly, this model would be sufficient to fly a real mission with a multiple-satellite-aided capture trajectory. In a real mission, however, none of these variables are known to perfect precision. Therefore, navigational errors must be taken into account. A full navigational analysis is beyond the scope of this paper; instead, we provide a rough sensitivity analysis of the flyby sequences. The "delta-Delta-v" navigation method is used to estimate the propagation of errors throughout the sequence.

Delta-Delta-V Flyby Navigation Method

We estimate the propagation of flyby errors using the delta-Delta-v method[17] by first calculating the equivalent ΔV of gravity assist flybys:

$$\Delta V_{\text{eq}} = \frac{2V_{\infty,\text{moon}}\mu_{\text{moon}}}{\mu_{\text{moon}} + V_{\infty,\text{moon}}^2(r_{\text{moon}} + h_{\text{p}})} \tag{13}$$

where ΔV_{eq} is the equivalent ΔV of the flyby, $V_{\infty,\text{moon}}$ is the hyperbolic excess velocity with respect to a moon, μ_{moon} is the gravitational parameter of a moon, r_{moon} is the physical radius of a moon, and h_{p} is the flyby altitude. The equivalent ΔV is computed for the nominal trajectory and for a perturbed trajectory that has a slightly different flyby altitude. The difference between the equivalent ΔV of the nominal trajectory and the perturbed trajectory is called the delta-Delta-v:

$$\delta(\Delta V) = \Delta V_{\text{eq,nom}} - \Delta V_{\text{eq,pert}} \tag{14}$$

where $\delta(\Delta V)$ is the variation of the ΔV caused by flyby error, $\Delta V_{\text{eq,nom}}$ is the equivalent ΔV of the nominal trajectory, and $\Delta V_{\text{eq,pert}}$ is the equivalent ΔV of the perturbed trajectory.

The B-plane error of the next flyby is computed by multiplying the delta-Delta-v by the time of flight of the transfer:

$$B_{\text{error}} = \delta(\Delta V)(T_{1,2}) \tag{15}$$

where B_{error} is the B-plane error in the second flyby and $T_{1,2}$ is the time of flight of the transfer between the two moons. If there is a third flyby in the sequence before JOI, the B-plane error can be used as the perturbation in the second flyby, and the B-plane error in the third flyby can be computed using the same method.

If JOI occurs in between flybys or before the entire sequence, we must account for the error in the JOI in the B-plane error calculations. We assume that the JOI manuever has a one-percent error in the worst direction (i.e. the direction that causes the error to compound with the flyby errors). Since the delta-Delta-v method is already a rough estimate, the fidelity is not significantly decreased when we merely add the B-plane error caused by the JOI to the B-plane error caused by the flybys:

$$B_{\text{error}} = \delta(\Delta V_{\text{flyby}})(T_{1,2}) + \delta(\Delta V_{\text{JOI}})(T_{\text{JOI},2}) \tag{16}$$

where $\delta(\Delta V_{\text{flyby}})$ is the variation of the flyby ΔV caused by the flyby error, $\delta(\Delta V_{\text{JOI}})$ is the variation of the JOI ΔV caused by the JOI error, and $T_{\text{JOI},2}$ is the time of flight of the transfer from perijove to the flyby after JOI.

This delta-Delta-v method is a very rough method for predicting errors, but it does provide some insight into which sequences are more difficult to navigate. It is also a purely ballistic method, so it does not take into account whether trajectory correction maneuvers could be executed in-between flybys of moons. The sequences that finish all of their flybys before JOI are also more operationally feasible than the others because the JOI maneuver is a mission-critical event.

DOUBLE-SATELLITE-AIDED CAPTURE RESULTS

Patched-Conic Double Satellite-Aided Capture

Capture sequences involving close flybys of two Galilean moons are collectively termed double-satellite-aided capture. For ballistic interplanetary trajectories from Earth, no double-flyby sequence can capture a spacecraft into Jupiter orbit without a JOI maneuver. Hence, each of these sequences must include a JOI maneuver in addition to the two flybys. Geometrically, double-flyby sequences only occur when the first moon is at a specific range of angles from the second moon. Noting that the moons are assumed to be in circular, coplanar orbits, opportunities only repeat every synodic period between the two moons:

$$S = \frac{2\pi}{n_1 - n_2} \tag{17}$$

where S is the synodic period, n_1 is the mean motion of the inner moon, and n_2 is the mean motion of the outer moon. For the Galilean moons of Jupiter, the mean motion of each moon and the synodic period between each set of moons are given in Table 2.

Table 2. Synodic Periods between Galilean Moons

Sequence	n_1 (deg/day)	n_2 (deg/day)	S (days)
Io-Europa	203.4890	101.3747	3.5255
Io-Ganymede	203.4890	50.3176	2.3503
Io-Callisto	203.4890	21.5711	1.9789
Europa-Ganymede	101.3747	50.3171	7.0509
Europa-Callisto	101.3747	21.5711	4.5111
Ganymede-Callisto	50.3176	21.5711	12.5232

The double satellite-aided capture trajectories that require the least ΔV are Io-Ganymede sequences because Io is deep in Jupiter's gravity well and Ganymede is the most massive moon in the Solar System. We divide these sequences into 4 different types based on the order of the flybys: Ganymede-Io-JOI (GIJ), Ganymede-JOI-Io (GJI), Io-JOI-Ganymede (IJG), and JOI-Io-Ganymede (JIG). Figure 2 shows an example IJG capture case.

All four Io-Ganymede sequences require approximately the same amount of ΔV_{JOI} to capture into a 200-day orbit. (All other capture sequences in this paper can be assumed to capture into 200-day orbits unless otherwise noted.) For radii of perijove above 4 R_{J}, these sequences require about 200 m/s less ΔV than equivalent single satellite-aided capture with either Io or Ganymede. Table 3 gives the ΔV_{JOI} for the Io- and Ganymede-aided capture, Io-aided capture, Ganymede-aided capture, and unaided capture for a range of perijoves.

A potential disadvantage of these Io-Ganymede sequences is that they all pass through Jupiter's harsh radiation environment near Io's orbit (at 5.9 R_{J}). For low-radiation capture with perijoves above 8 R_{J}, Ganymede-Callisto sequences are the most efficient double-satellite-aided-capture sequences. Table 4 gives the ΔV_{JOI} for Ganymede- and Callisto-aided capture, Ganymede-aided capture, Callisto-aided capture, and unaided capture at perijoves above 8 R_{J}.

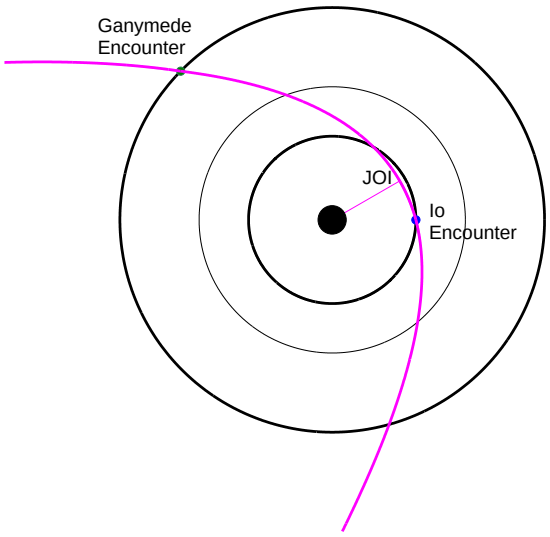

Figure 2 Io-JOI-Ganymede sequence with a perijove of 5.5 R_J, a V_∞ of 5.6 km/s, flyby altitudes of 300 km, and a ΔV_{JOI} of 370 m/s.

Table 3. ΔV for Io and Ganymede Capture Sequences,[a] m/s

Flyby Sequences	JOI(5 R_J) ΔV, m/s	JOI(4 R_J) ΔV, m/s	JOI(3 R_J) ΔV, m/s	JOI(2 R_J) ΔV, m/s	JOI(1.01 R_J) ΔV, m/s
Unaided	825	735	641	524	371
Ganymede	630	573	507	425	308
Io	556	526	483	416	311
GIJ	349	355	346	311	242
GJI	337	349	342	309	240
IJG	345	350	342	309	240
JIG	330	340	333	299	228

[a] V_∞ is 5.6 km/s and flyby altitudes are 300 km.

Table 4. ΔV for Ganymede and Callisto Capture Sequences[a], m/s

Flyby Sequences	JOI(14 R_J) ΔV, m/s	JOI(13 R_J) ΔV, m/s	JOI(12 R_J) ΔV, m/s	JOI(11 R_J) ΔV, m/s	JOI(10 R_J) ΔV, m/s	JOI(9 R_J) ΔV, m/s
Unaided	1366	1317	1267	1215	1160	1101
Ganymede	962	863	830	810	791	771
Callisto	1084	1054	1021	985	948	904
CGJ	646	567	555	556	559	558
CJG	528	508	518	529	538	540
GJC	620	550	539	541	544	544
JGC	519	498	506	517	526	529

[a] V_∞ is 5.6 km/s and flyby altitudes are 300 km.

Three of the remaining types of sequences—Ganymede-Europa sequences, Io-Europa sequences, and Io-Callisto sequences—cost more ΔV than Io-Ganymede sequences and Ganymede-Callisto sequences, but they still cost substantially less ΔV than single satellite-aided capture at Io. The ΔV costs of Europa-Callisto sequences are comparable to Io-aided capture.

Integrated Double-Satellite-Aided Capture

Double-satellite-aided capture sequences involve the targeting of only four B-plane parameters (two for each moon) and the final C3 energy, so the four available hyperbolic asymptote control variables (I.C.'s) and an anti-velocity-vector JOI control variable are sufficient to converge every double-satellite-aided capture sequence. From a computational perspective, the order of the double-flyby sequences is more important than the set of two moons chosen. The three possible double-flyby sequences are: both moons then JOI, JOI in between moon flybys, and JOI then both flybys.

Table 5. Double Flyby Sequence Targeting

Sequence Type	Event 1	Event 2	Event 3	Event 4	Event 5
Moon-Moon-JOI	I.C.'s (4 C)	Flyby 1 B-plane(2 T)	Flyby 2 B-plane(2 T)	JOI (1 C)	C3(1 T)
Moon-JOI-Moon	I.C.'s (4 C)	Flyby 1 B-plane(2 T)	JOI (1 C)	Flyby 2 B-plane(2 T)	C3(1 T)
JOI-Moon-Moon	I.C.'s (4 C)	JOI (1 C)	Flyby 1 B-plane(2 T)	Flyby 2 B-plane(2 T)	C3(1 T)

Since both sets of B-plane parameters can always be precisely targeted, all such double-flyby sequences are considered to be optimal. Because these solutions are optimal, the ΔV_{JOI} required is approximately equivalent to the patched-conic estimates. The target radius of perijove and target C3 energy can also be manually modified to get the desired closest approach distance to Jupiter and final orbit shape. These manual modifications, particularly the modification of the target perijove, also increase the range of potential interplanetary trajectories that are available to these double-flyby sequences.

We analyze the interplanetary flyby windows of several double-satellite-aided capture sequences by converging several trajectories, recording their RA, and determining the RA that corresponds to a Hohmann trajectory. The RA is useful because it provides the angle of the incoming V_∞ vector of the capture sequence with respect to a Jupiter-fixed frame. We then compare the recorded RA from a double-satellite-aided capture sequence with the RA of a Hohmann transfer from Earth at that particular date. If the RA of the trajectory is close to the RA for a Hohmann trajectory, then it is possible to find an interplanetary trajectory that will align with the double-satellite-aided capture sequence. We note that any of the triple- or quadruple-satellite-aided capture sequences presented later in this paper correspond to special cases of this analysis (i.e. a single RA angle in the graph), so each of those trajectories only has about a 1 in 18 chance (within $\pm 10^\circ$ of the Hohmann angle out of 360° of possible RA values) of aligning with an optimal interplanetary trajectory.

We choose two double-satellite-aided capture trajectories for each window: a trajectory that is close to the maximum possible perijove (i.e. the orbital radius of the moon closest to Jupiter in that sequence) and a trajectory that is close to the minimum possible perijove (the physical radius of Jupiter). All other trajectories that are within the window have perijoves, RA, and perijove times that are between these two extrema. The two extreme trajectories for the second window are found by increasing the initial time of each of the original extreme trajectories by one synodic period of the two moons (see Table 2) and re-converging. We repeat this process until we can deduce the behavior of the particular type of double-satellite-aided capture sequence (e.g. Ganymede-Io-JOI).

Interplanetary flyby windows for Ganymede and Io double-satellite-aided capture. Figure 3 is a polar plot of the RA angles of each of six successive interplanetary windows. The plot shows that there are three distinct flyby windows every Ganymede orbital period. The mismatch between the period of Ganymede (7.1546 days) and three times the synodic period of Io and Ganymede (7.0509 days) causes a RA offset of about five degrees every three windows.

Since the first three windows span 90 degrees of RA and about 15 more degrees are spanned every additional seven days, the entire 360 degrees of RA will be spanned in about 18 weeks. Since we are using a Jupiter-centered coordinate frame rather than a heliocentric frame, the Hohmann angle varies by 360 degrees every Jupiter orbital period of 11.9 years. This effect means that the Hohmann angle will change by about 10 degrees over the 18 weeks. The Hohmann angle changes in the opposite direction from the window offset, so it effectively reduces the amount of time required to ensure that an interplanetary trajectory will occur to about 16 weeks.

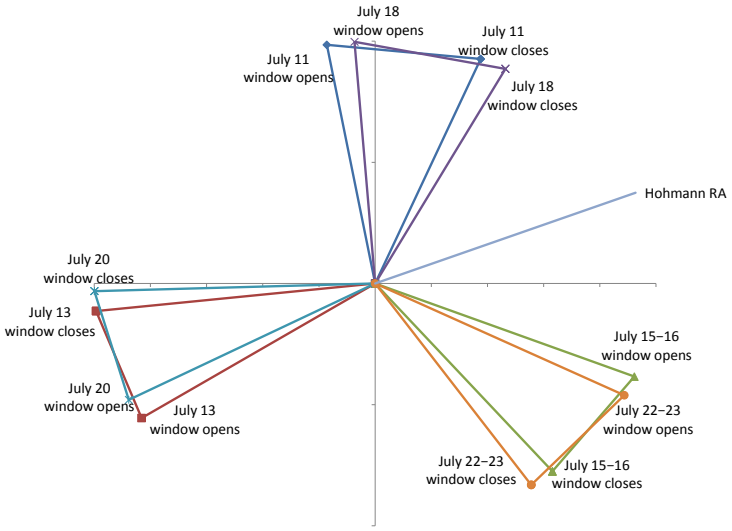

Figure 3 Polar plot of the RA angles of Ganymede-Io-JOI flyby windows. The Hohmann RA angle is not encompassed by a petal, so a Ganymede-Io-JOI capture sequence is not available for an interplanetary trajectory from Earth during this arrival time frame. The petals rotate about 6 degrees every week, so a Ganymede-Io-JOI sequence will become available in about 8 weeks.

Another Ganymede and Io sequence, Ganymede-JOI-Io, has a much larger range of available interplanetary trajectories because about 270 degrees of the 360 degrees of RA are spanned at any given time. The remaining RA angles would be able to be spanned about 6 weeks after the original time. We plot a polar plot of the Ganymede-JOI-Io sequence in Figure 4.

Interplanetary Windows for the Callisto-Ganymede-JOI sequence. The Callisto-Ganymede-JOI sequence has somewhat different behavior from the Ganymede-Io-JOI sequences because of the dynamics of Ganymede and Callisto. The orbital period of Callisto (16.69 days), the synodic period of Callisto and Ganymede (12.52 days), and the orbital period of Ganymede (7.155 days) are very close to a 3:4:7 resonance with a near-resonance period of approximately 50 days. Hence, Figure 5 shows a barely recognizable change in the windows that corresponds to about 0.5 degrees every 50 days. However, the Hohmann angle changes by about 4 degrees during that same time period. Thus, the motion of Jupiter's orbit around the Sun dominates the mismatch between flybys for a Callisto-Ganymede-JOI case. We observe 4 "petals" on the polar plot (each spanning about 30–40 degrees), so about 140 degrees of RA are spanned at any given time. However, a flyby sequence is not possible unless the Hohmann angle is encompassed by a petal (which will occur in at most two years in Figure 5).

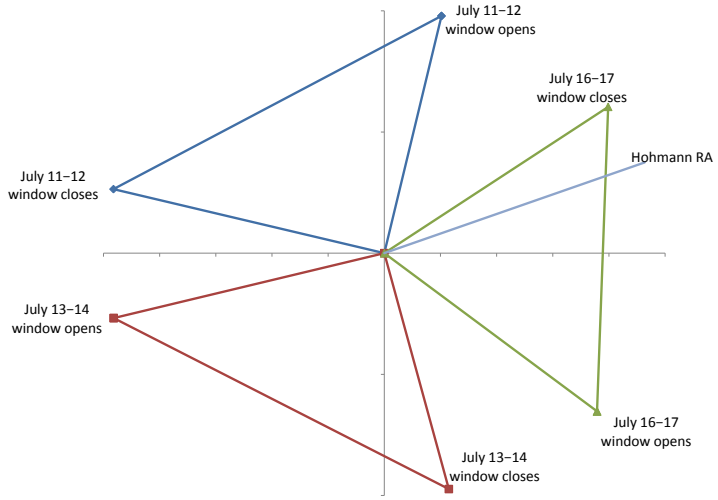

Figure 4 Polar plot of the RA angles of Ganymede-JOI-Io flyby windows. In this example, the Hohmann RA angle is contained in one of the petals, so a Ganymede-JOI-Io capture sequence is available for an interplanetary trajectory from Earth.

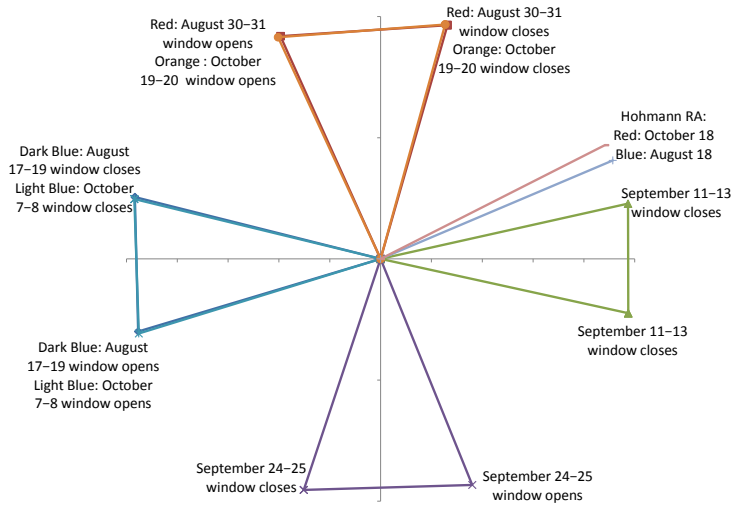

Figure 5 Polar plot of the RA angles of Callisto-Ganymede-JOI flyby windows. In this case, the petals are separated by about 12.5 days and the angles nearly repeat every 50 days. The Hohmann RA rotates about 5 degrees every 2 months, so the next Callisto-Ganymede-JOI flyby sequence that is available for an interplanetary transfer from Earth occurs after nearly two years.

Double Flyby Navigation Results

We apply the delta-Delta-v method to double-satellite-aided capture trajectories to determine which trajectories are the most feasible in terms of navigation. The most delta-v optimal cases, Ganymede and Io double flyby sequences, are tabulated in Table 6. The most radiation tolerant sequences, Callisto and Ganymede double-flyby sequences, are tabulated in Table 7. These results show that the flyby sequences that do not have a JOI manuever before flybys are the most "navigationally feasible" if the trajectories are propagated ballistically with no trajectory correction maneuvers.

Table 6 Error due to a 10-km Flyby Error in the First Flyby on the Second Flyby with JOI errors of 1%, km.

Perijove (R_J)	5	4	3	2	1
GIJ Io flyby error	82	69	60	53	47
GJI Io flyby error	140	150	150	130	110
IJG Ganymede flyby error	300	280	250	220	170
JIG Ganymede flyby error	370	350	300	230	150

Table 7 Error due to a 10-km Flyby Error in the First Flyby on the Second Flyby with JOI errors of 1%, km.

Perijove (R_J)	14	13	12	11	10	9
CGJ Ganymede flyby error (km)	240	210	180	170	150	140
CJG Ganymede flyby error (km)	530	600	650	680	700	700
GJC Callisto flyby error (km)	1500	1400	1400	1300	1300	1300
JGC Callisto flyby error (km)	6100	6300	6300	6100	5800	5400

TRIPLE SATELLITE-AIDED CAPTURE

Laplace Resonance Derivation

Ganymede, Europa, and Io are locked in a 1:2:4 orbital resonance known as the Laplace resonance.[12] The Laplace resonance constrains the three moons's mean longitudes[14,15] by the relation:

$$180^\circ = 2\lambda_{\mathrm{Ga}} - 3\lambda_{\mathrm{Eu}} + \lambda_{\mathrm{Io}} \tag{18}$$

where λ_{Io} is Io's mean longitude, λ_{Eu} is Europa's mean longitude, and λ_{Ga} is Ganymede's mean longitude.

The Laplace resonance constrains the geometry of triple-satellite-aided capture trajectories involving Ganymede, Europa, and Io such that some potential sequences cannot exist. However, the triple-flyby sequences that do exist repeat every synodic period of Europa and Ganymede (7.0509 days). We determine which Laplacian triple-flyby sequences can physically exist by performing a detailed phase angle analysis combined with the patched-conic method previously discussed.

The Laplace resonance is the combined effect of several resonances. The following mean motion and phasing resonances constrain the dynamics and positions of Io and Europa as follows:[14]

$$2n_{Eu} - n_{Io} = \dot{\varpi}_{\mathrm{Io}} = \dot{\varpi}_{\mathrm{Eu}} \approx -0.7395^\circ/\mathrm{day} \tag{19}$$

$$2\lambda_{\mathrm{Eu}} - \lambda_{\mathrm{Io}} - \varpi_{\mathrm{Io}} = 0^\circ \tag{20}$$

$$2\lambda_{\mathrm{Eu}} - \lambda_{\mathrm{Io}} - \varpi_{Eu} = 180^\circ \tag{21}$$

where n_{Io} is Io's mean motion, n_{Eu} is Europa's mean motion, ϖ_{Io} is Io's longitude of perijove, ϖ_{Eu} is Europa's longitude of perijove, $\dot{\varpi}_{\text{Io}}$ is the precession rate of Io's longitude of perijove, and $\dot{\varpi}_{\text{Eu}}$ is the precession rate of Europa's longitude of perijove.

Similarly, Europa and Ganymede are locked in a 1:2 orbital resonance with each other. In this case, only Europa's longitude of perijove participates in the resonance, while Ganymede's longitude of perijove is not constrained.

$$2n_{\text{Ga}} - n_{\text{Eu}} = \dot{\varpi}_{\text{Eu}} \approx -0.7395^{\circ}/\text{day} \tag{22}$$

$$2\lambda_{\text{Ga}} - \lambda_{\text{Eu}} - \varpi_{\text{Eu}} = 0^{\circ} \tag{23}$$

where n_{Ga} is the mean motion of Ganymede and the other parameters have all been previously defined in Equations (18) – (21). The Laplace resonance mean motion equation is derived by subtracting Equation (19) from Equation (22).

$$2n_{\text{Ga}} - 3n_{\text{Eu}} + n_{\text{Io}} = 0 \tag{24}$$

We derive the Laplace resonance phasing equation by subtracting Equation (21) from Equation (23) (where we note that any odd integer multiple of 180° will satisfy the equation):

$$m(180^{\circ}) = 2\lambda_{\text{Ga}} - 3\lambda_{\text{Eu}} + \lambda_{\text{Io}} \tag{25}$$

where m is any odd integer ($m = ..., -3, -1, 1, 3, ...$). Subtracting Equation (20) from Equation (21) shows that the longitudes of perijove of Europa and Io are locked in a separate resonance:

$$\varpi_{\text{Io}} = 180^{\circ} - \varpi_{\text{Eu}} \tag{26}$$

Laplace Resonance Phase Angle Analysis

The geometry of the Laplace resonance allows the position of any moon to be determined from the angle between the other two moons (the phase angle). We define the phase angles between each set of moons as the difference between the mean longitudes of each moon at a given time:

$$\Delta\lambda_{\text{Eu,Io}} \equiv \lambda_{\text{Io}} - \lambda_{\text{Eu}} \tag{27}$$

$$\Delta\lambda_{\text{Ga,Io}} \equiv \lambda_{\text{Io}} - \lambda_{\text{Ga}} \tag{28}$$

$$\Delta\lambda_{\text{Ga,Eu}} \equiv \lambda_{\text{Eu}} - \lambda_{\text{Ga}} \tag{29}$$

where $\Delta\lambda_{\text{Eu,Io}}$ is the phase angle from Europa to Io; $\Delta\lambda_{\text{Ga,Io}}$ is the phase angle from Ganymede to Io; $\Delta\lambda_{\text{Ga,Eu}}$ is the phase angle from Ganymede to Europa; and λ_{Io}, λ_{Eu}, and λ_{Ga} are the mean longitudes of Io, Europa, and Ganymede, respectively. Next, we manipulate the Laplace resonance phasing equation to form relations between each set of phase angles.

Ganymede-Europa and Europa-Io phase angle relations. The relations between the phase angle between Ganymede and Europa and the phase angle between Europa and Io are determined by first re-arraging terms in Equation (18) to get

$$\pm 180^\circ = 2\lambda_{\text{Ga}} - 2\lambda_{\text{Eu}} + \lambda_{\text{Io}} - \lambda_{\text{Eu}} \tag{30}$$

where the $\pm$ symbols denote two solutions. Equations (27) and (29) are substituted into Equation (30) to form a relation between the two sets of phase angles:

$$\pm 180^\circ = -2\Delta\lambda_{\text{Ga,Eu}} + \Delta\lambda_{\text{Eu,Io}} \tag{31}$$

We rearrange Equation (31) to solve for each phase angle in terms of the other:

$$\Delta\lambda_{\text{Eu,Io}} = 180^\circ + 2\Delta\lambda_{\text{Ga,Eu}} \tag{32}$$

$$\Delta\lambda_{\text{Ga,Eu}} = \pm 90^\circ + \Delta\lambda_{\text{Eu,Io}}/2 \tag{33}$$

where the $\pm$ terms imply that there exist two possible $\Delta\lambda_{\text{Ga,Eu}}$ solutions for a given value of $\Delta\lambda_{\text{Eu,Io}}$ due to the fact that $\Delta\lambda_{\text{Eu,Io}}$ varies from 0° to 360° twice every period of the Laplace resonance while $\Delta\lambda_{\text{Ga,Eu}}$ varies at the same angular rate as the Laplace resonance.

Ganymede-Europa and Ganymede-Io phase angle relations. The Laplace resonance equation [Equation (25)] with odd multiples of 180° is rearranged to form

$$\{\pm 180^\circ, 540^\circ\} = 2\lambda_{\text{Ga}} - 3\lambda_{\text{Eu}} + \lambda_{\text{Io}} \tag{34}$$

where $\{\pm 180^\circ, 540^\circ\}$ represents three odd multiples of 180° that are required to span the solution space. Equation (28) is rearranged in terms of λ_{Io} as follows:

$$\lambda_{\text{Io}} = \Delta\lambda_{\text{Ga,Io}} + \lambda_{\text{Ga}} \tag{35}$$

Next, Equation (35) is substituted into Equation (34) to obtain

$$\{\pm 180^\circ, 540^\circ\} = 3\lambda_{\text{Ga}} - 3\lambda_{\text{Eu}} + \Delta\lambda_{\text{Ga,Io}} \tag{36}$$

where $3\lambda_{\text{Ga}} - 3\lambda_{\text{Eu}}$ can be replaced by $-3\Delta\lambda_{\text{Ga,Eu}}$ via Equation (29) to form

$$\{\pm 180^\circ, 540^\circ\} = -3\Delta\lambda_{\text{Ga,Eu}} + \Delta\lambda_{\text{Ga,Io}} \tag{37}$$

Equation (37) is rearranged to solve for each phase angle in terms of the other. Remaining odd multiples of 180° are then replaced by 180° to condense the equations. These operations result in the following:

$$\Delta\lambda_{\text{Ga,Io}} = 3\Delta\lambda_{\text{Ga,Eu}} + 180^\circ \tag{38}$$

$$\Delta\lambda_{\text{Ga,Eu}} = \{\pm 60^\circ, 180^\circ\} + \Delta\lambda_{\text{Ga,Io}}/3 \tag{39}$$

where the braced terms and the $\pm$ denote three solutions for $\Delta\lambda_{\text{Ga,Eu}}$ for a given value of $\Delta\lambda_{\text{Ga,Io}}$. The three solutions exist due to the fact that $\Delta\lambda_{\text{Ga,Io}}$ varies from 0° to 360° three times every period of the Laplace resonance while $\Delta\lambda_{\text{Ga,Eu}}$ varies at the same angular rate as the Laplace resonance.

Ganymede-Io and Europa-Io phase angle relations. We determine the relations between the Ganymede-Io phase angle and the Europa-Io phase angle by using a substitution for λ_{Eu} that is derived by rearranging Equation (27):

$$\lambda_{\text{Eu}} = \lambda_{\text{Io}} - \Delta\lambda_{\text{Eu,Io}} \tag{40}$$

Equation (40) is next substituted into the three-valued form of the Laplace resonance equation [Equation (34)]:

$$\{\pm 180^\circ, 540^\circ\} = 2\lambda_{\text{Ga}} - 2\lambda_{\text{Io}} + 3\Delta\lambda_{\text{Eu,Io}} \tag{41}$$

where $2\lambda_{\text{Ga}} - 2\lambda_{\text{Io}}$ can be replaced by $-2\Delta\lambda_{\text{Ga,Io}}$ via Equation (28) to form

$$\{\pm 180^\circ, 540^\circ\} = -2\Delta\lambda_{\text{Ga,Io}} + 3\Delta\lambda_{\text{Eu,Io}} \tag{42}$$

This equation is rearranged to solve for each of phase angle in terms of the other:

$$\Delta\lambda_{\text{Eu,Io}} = \{\pm 60^\circ, 180^\circ\} + 2\Delta\lambda_{\text{Ga,Io}}/3 \tag{43}$$

where the braced terms and the $\pm$ denote three solutions for $\Delta\lambda_{\text{Ga,Eu}}$ for a given value of $\Delta\lambda_{\text{Ga,Io}}$.

$$\Delta\lambda_{\text{Ga,Io}} = \pm 90^\circ + 3\Delta\lambda_{\text{Eu,Io}}/2 \tag{44}$$

where the $\pm$ denotes two solutions for $\Delta\lambda_{\text{Ga,Io}}$ for a given value of $\Delta\lambda_{\text{Ga,Eu}}$. These two sets of multi-valued solutions occur because $\Delta\lambda_{\text{Ga,Io}}$ varies from 0° to 360° three times every period of the Laplace resonance while $\Delta\lambda_{\text{Ga,Eu}}$ varies two times every period of the Laplace resonance. Interestingly, given any of the three possible values of $\Delta\lambda_{\text{Ga,Io}}$, the relations can produce either of the two possible values of $\Delta\lambda_{\text{Ga,Eu}}$. Similarly, given either of the two possible values of $\Delta\lambda_{\text{Ga,Eu}}$, the relations can produce any of the three possible values of $\Delta\lambda_{\text{Ga,Io}}$.

Dynamics of the Laplace Resonance. The mean motion of the moons governs the dynamics of the Laplace resonance by varying the mean longitudes over time. The mean longitudes of each moon can be written as a function of time. After one full period of the Laplace resonance (7.0509 days), the angles can be reset to their initial values:

$$\lambda_{\text{Io}}(t) = \lambda_{\text{Io},0} + n_{\text{Io}}t \tag{45}$$

$$\lambda_{\text{Eu}}(t) = \lambda_{\text{Eu},0} + n_{\text{Eu}}t \tag{46}$$

$$\lambda_{\text{Ga}}(t) = \lambda_{\text{Ga},0} + n_{\text{Ga}}t \tag{47}$$

where $\lambda_{\text{Io}}(t)$, $\lambda_{\text{Eu}}(t)$, and $\lambda_{\text{Ga}}(t)$ are the mean longitudes of the moons at time t; and $\lambda_{\text{Io},0}$, $\lambda_{\text{Eu},0}$, and $\lambda_{\text{Ga},0}$ are arbitrary initial conditions for the mean longitudes of the moons that satisfy the Laplace resonance equation [Equation (25)].

We determine the phase angles between each set of moon over time, by finding the differences between Equations (45) – (47). These time-varying phase angles can also be written in terms of the initial phase angles and the differences in the mean motions of the moons:

$$\Delta\lambda_{\text{Eu,Io}}(t) = \lambda_{\text{Io}}(t) - \lambda_{\text{Eu}}(t) = \Delta\lambda_{\text{Eu0,Io0}} + (n_{\text{Io}} - n_{\text{Eu}})t \tag{48}$$

$$\Delta\lambda_{\text{Ga,Io}}(t) = \lambda_{\text{Io}}(t) - \lambda_{\text{Ga}}(t) = \Delta\lambda_{\text{Ga0,Io0}} + (n_{\text{Io}} - n_{\text{Ga}})t \tag{49}$$

$$\Delta\lambda_{\text{Ga,Eu}}(t) = \lambda_{\text{Eu}}(t) - \lambda_{\text{Ga}}(t) = \Delta\lambda_{\text{Ga0,Eu0}} + (n_{\text{Eu}} - n_{\text{Ga}})t \tag{50}$$

where $\Delta\lambda_{\text{Eu,Io}}(t)$, $\Delta\lambda_{\text{Ga,Io}}(t)$, and $\Delta\lambda_{\text{Ga,Eu}}(t)$ are the time-varying phase angles between each set of moons; $\Delta\lambda_{\text{Eu0,Io0}}$, $\Delta\lambda_{\text{Eu0,Io0}}$, and $\Delta\lambda_{\text{Eu0,Io0}}$ are the initial phase angles between the moons that are constrained by Equations (32) – (39); and t is the time elapsed after the initial phase angles occur.

Given the difference between the mean longitudes of any two moons at two known times, the phase angles between all three moons can be calculated for both times. We apply this technique to the Laplace triple-satellite-aided capture problem by determining the position of the third moon after the first two moon flybys and analyzing if the trajectory passes near it. The phase angle between a set of moons at two different times is defined using the time of flight of the spacecraft as it transfers from one moon to the other:

$$\Delta f_{\text{Eu,Io}} = \Delta\lambda_{\text{Eu1,Io2}} = \lambda_{\text{Io}}(t_2) - \lambda_{\text{Eu}}(t_1) = \lambda_{\text{Io},1} + n_{\text{Io}}(T_{1,2}) - \lambda_{\text{Eu},1} \tag{51}$$

where $\Delta f_{\text{Eu,Io}}$ is the difference of the true anomalies of Europa and Io calculated from Equations (4) – (5), $\Delta\lambda_{\text{Eu1,Io2}}$ is the phase angle from Europa at time t_1 to Io at time t_2, and $T_{1,2}$ is the time of flight from the outer moon to the inner moon. If Ganymede and Io are encountered first, we substitute Ga for Eu in the expression. Similarly, if Ganymede and Europa are encountered first, we substitute Ga for Eu and Eu for Io in the expression. For sequences that begin past the spacecraft's perijove, the phase angles between each inner moon at time t_1 to each outer moon at time t_2 can be calculated using the same method.

The primary advantage of these relations is that the phase angle difference is equivalent to the difference of the true anomalies of the moons that we calculated earlier in Equations (4) – (5). Hence, the phase angle relations that were derived from the Laplace's astronomical research[12] can be applied to the trajectory design of the moon-to-moon transfers of triple-satellite-aided capture sequences. All that remains to be determined is the initial phase angle of the third moon. We can determine this angle from the phase angle between the first two moon encounters by using the mean motion and time of flight relations. First, the phase angles of all three moons at both times need to be determined:

$$\Delta\lambda_{\text{Eu1,Io1}} = \Delta\lambda_{\text{Eu1,Io2}} - n_{\text{Io}}(T_{1,2}) \tag{52}$$

$$\Delta\lambda_{\text{Eu2,Io2}} = \Delta\lambda_{\text{Eu1,Io1}} + (n_{\text{Io}} - n_{\text{Eu}})(T_{1,2}) \tag{53}$$

Once the Europa-Io phase angles at both times are calculated, the Ganymede-Io and Ganymede-Europa phase angles can be determined using Equations (33) and (44). Similarly, if the Ganymede-Io or Ganymede-Europa phase angles at different times are given, Equations (52) and (53) are modified to calculate the phase angles at both times. Next, Equations (32), (38), (39), and (43) are used to calculate the remaining phase angles.

Finally, the time of flight from the second moon to the third moon at two different times is used to determine the third moon's phase angle at the time that the spacecraft passes its orbit:

$$\Delta\lambda_{\text{Ga3,Io2}} = \Delta\lambda_{\text{Ga2,Io2}} - n_{\text{Ga}}(T_{2,3}) \tag{54}$$

If this phase angle is equal to the difference in the true anomalies of the two encounters, then the triple-satellite-aided capture sequence is physically possible:

$$\Delta\lambda_{\text{Ga3,Io2}}(\mathcal{E}_{in}, R_{\text{p,in}}) = \Delta f_{\text{Ga3,Io2}}(\mathcal{E}_{in}, (R_{\text{p,in}})) \tag{55}$$

Both angles are determined by the same set of initial conditions, the input orbital energy (or V_∞) and target perijove. If the angles are not the same, both parameters will have to be varied until the equality is met. For the multi-valued phase angle functions, only one of the phase angles must be equal to the difference in the true anomalies.

The V_∞ range is constrained by the set of possible interplanetary trajectories from Earth to Jupiter. We search a V_∞range from 0 km/s to 7 km/s to account for the majority of ballistic interplanetary trajectories and low-thrust trajectories which can arrive at Jupiter with low V_∞ or even elliptical orbits.[11] Similarly, we constrain the target perijove so that it is above Jupiter's surface (1 R_J) and below Io's orbit (5.9 R_J). If no trajectory can be found for a particular sequence throughout the entire range, the capture sequence is considered to be physically impossible.

Patched-Conic, Laplacian Triple-Satellite-Aided Capture Results

We determine the potential Laplacian triple-satellite-aided capture sequences by analyzing possible sequences that contain a JOI maneuver at perijove and flybys of Io, Europa, and Ganymede. Each of these sequences is then tested using the Laplace resonance phase angle analysis from the previous section. If a sequence exists, its required perijove and JOI delta-v are recorded. Otherwise, the sequence is recorded as an impossible sequence.

Table 8. Laplace Resonance Capture Sequences[a]

Flyby Sequences	Existence	Uniqueness	JOI ΔV, m/s	Perijove Radius, R_J
GEIJ	No	—	—	—
GEJI	Yes	Yes	213	1.15
GIJE	Yes	Yes	254	2.16
GJIE	No	—	—	—
EIJG	No	—	—	—
EJIG	Yes	Yes	244	2.11
IJEG	Yes	Yes	245	1.15
JIEG	No	—	—	—

[a] V_∞ is 5.6 km/s and flyby altitudes are 300 km.

Table 8 shows that only half of the potential Laplace resonance flyby sequences are physically realizable, and these sequences all have very low perijoves that are deep within Jupiter's radiation zone. It should also be noted that all of the physically possible sequences have a JOI manuever between the moon flybys, which poses navigational and operational challenges.

Figure 6 shows a possible Ganymede-Io-JOI-Europa (GIJE) sequence, while Figure 7 shows why Ganymede-Europa-Io-JOI (GEIJ) sequences are impossible—Io will always be on the other side of Jupiter from its required position. No amount of varying the incoming V_∞ or target perijove will modify the trajectory substantially enough overcome this problem. The geometry of the Laplace resonance definitively precludes this flyby sequence from existing.

The two sequences shown in Figures 6 and 7 have symmetric sequences with similar characteristics that are palindromes of the the original sequences. For instance, the GIJE and EJIG sequences are similar in perijove radius and geometry; the GEJI and IJEG sequences are also similar in perijove radius and geometry. The two sets of impossible sequences also occur in palindrome pairs: GEIJ and JIEG, and EIJG and GJIE. This property is due to the fact that all of the trajectories capture into long-period, 200-day orbits that are qualitatively similar to the hyperbolic arrival asymptotes.

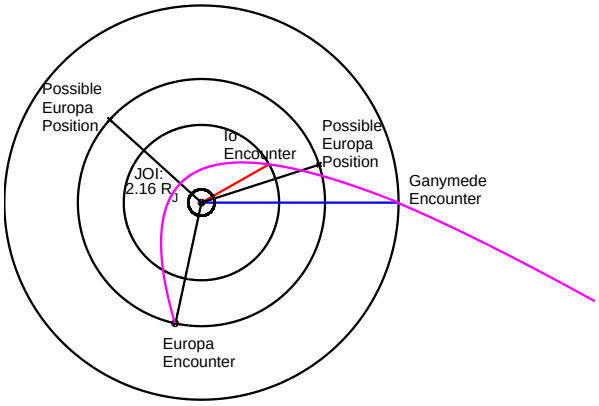

Figure 6 A Ganymede-Io-JOI-Europa sequence with a perijove of 2.16 $R_{\mathbf{J}}$, a V_∞ of 5.6 km/s, flyby altitudes of 300 km, and a $\Delta V_{\mathbf{JOI}}$ of 213 m/s. The Laplace resonance permits two other positions for Europa, but neither results in an encounter.

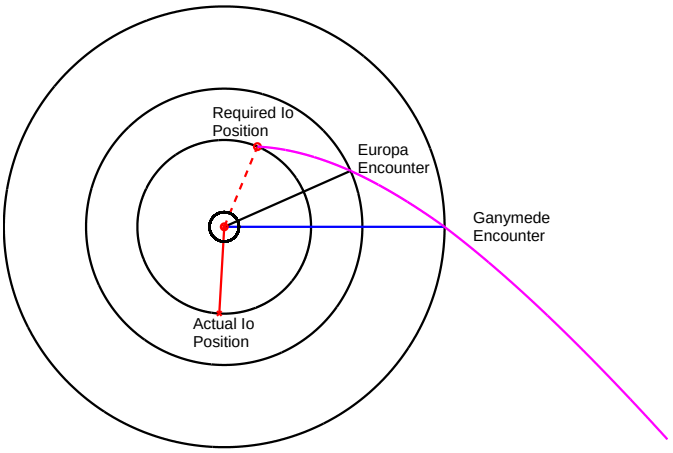

Figure 7 This Ganymede-Europa-Io-JOI flyby sequence is physically impossible because Io will always be located on the opposite side of Jupiter from where the trajectory passes Io's orbit. Varying the V_∞ or perijove does not change this conclusion.

Near Resonance Analysis for Callistan Triple-Satellite Aided Capture

Callisto is not in an exact resonance with the three other moons, so triple-satellite-aided capture sequences involving Callisto occur aperiodically rather than every 7.055 days. However, near-resonances can be found in the synodic periods of the tranfers that allow some prediction of when Callistan triple-satellite-aided capture can occur. Fortuitously, the synodic period of a Callisto-Ganymede transfer is nearly commensurate with the synodic period of a Ganymede-Io transfer:

$$\frac{S_{\text{Ca,Ga}}}{S_{\text{Ga,Io}}} = \frac{12.5232 \text{ days}}{2.3503 \text{ days}} = 5.3283 \approx 5.3333... = \frac{16}{3} \tag{56}$$

where $S_{\text{Ca,Ga}}$ is the synodic period of a Callisto-Ganymede transfer, $S_{\text{Ga,Io}}$ is the synodic period of a Ganymede-Io transfer, and 16/3 is the lowest near-resonance to the ratio of the synodic periods. Since this resonance is imperfect, there is a mismatch every period of the resonance:

$$M_{\text{Ca,Ga,Io}} = 16S_{\text{Ga,Io}} - 3S_{\text{Ca,Ga}} = 0.0352 \text{ days} \tag{57}$$

where $M_{\text{Ca,Ga,Io}}$ is the mismatch time in the near resonance per resonance period. This value can be multiplied by Callisto's mean motion and Callisto's orbital circumference to determine the approximate mismatch distance:

$$x_{\text{Ca,Ga,Io}} \approx M_{\text{Ca,Ga,Io}} n_{\text{Ca}} (2\pi a_{\text{Ca}}) = 24900 \text{ km} \tag{58}$$

where $x_{\text{Ca,Ga,Io}}$ is the approximate mismatch distance between the position of Callisto after one period of the near resonance, n_{Ca} is the mean motion of Callisto, and a_{Ca} is the semi-major axis of Callisto's orbit.

The mismatch can be corrected by varying the perijove of the sequence. However, the perijove can only be varied between Jupiter's surface (1 R_{J}) and Io's orbital semi-major axis(5.9 R_{J}) which limits the solution space of available trajectories. Callisto-Ganymede-Io-JOI and JOI-Io-Ganymede-Callisto trajectories occur for several near resonance periods producing a "flyby window," then no trajectory of that type will exist until the next flyby window. This behavior is due to the fact that these trajectories have three flybys in a row before or after perijove, so small variations in perijove only produce small variations in the B-plane parameters of the next flyby.

The next flyby window occurs when the near-resonance mismatches compound for so long that they become greater than one-sixteenth of Callisto's orbital circumference. This allows the next flyby window to open with a $\pm S_{\text{Ga,Io}}$ offset from the previous near-resonance period. We estimate the time between the beginning of one flyby window and the beginning of the next by multiplying the approximate near-resonance period by one-sixteenth of Callisto's orbital circumference, and dividing by the mismatch distance:

$$S_{\text{Ca,Ga,Io}} \approx \frac{16S_{\text{Ga,Io}}(2\pi a_{\text{Ca}}/16)}{x_{\text{Ca,Ga,Io}}} = 1110 \text{ days} = 3.05 \text{ years} \tag{59}$$

where $S_{\text{Ca,Ga,Io}}$ is the approximate "synodic period" between the two Callisto-Ganymede-Io-JOI (or JOI-Io-Ganymede-Callisto) trajectories with approximately equivalent perijoves.

On the other hand, Callisto, Ganymede, and Io sequences that have JOI in-between flybys allow a small variation in perijove to cause a much greater variation the B-plane parameters of the next flyby. Consequently, these trajectories occur much more frequently, once or twice every near-resonance period.

Patched-Conic Callistan-Triple-Satellite-Aided Capture Results

The aperiodicity also allows all Callistan triple-satellite-aided capture sequences to exist (unlike some of the Laplacian sequences), and also allows a broader range of perijove distances. We employ a similar patched-conic method to that of the double-satellite-aided capture sequences to determine the ΔV required

for Callistan triple-satellite-aided capture sequences. The only difference is that an additional flyby is modeled, so the capture ΔV is lower.

The Callistan triple-satellite-aided capture sequences that require the least ΔV are Callisto-Ganymede-Io sequences. These sequences take advantage of Io's position deep within Jupiter's gravity well and the large masses of Ganymede and Callisto. (Ganymede and Callisto are the first and third most massive moons in the Solar System, respectively.) We list the eight different permutations for Callisto-Ganymede-Io flyby sequences and their ΔV versus perijove in Table 9.

Table 9. ΔV for Callisto, Ganymede, and Io Capture Sequences[a], m/s

Flyby Sequences	JOI (5 R_J) ΔV, m/s	JOI (4 R_J) ΔV, m/s	JOI (3 R_J) ΔV, m/s	JOI (2 R_J) ΔV, m/s	JOI (1.01 R_J) ΔV, m/s
CGIJ	208	236	248	236	191
CGJI	203	234	247	236	191
CIJG	211	236	248	236	191
CJIG	205	234	247	235	191
GIJC	207	233	246	234	190
GJIC	202	232	245	234	190
IJGC	210	234	246	234	190
JIGC	204	232	245	234	190

[a] V_∞ is 5.6 km/s and flyby altitudes are 300 km.

The Callisto-Ganymede-Io sequences encounter the same radiation field as all of the other Io sequences, so a method of avoiding radiation is to use Callisto-Ganymede-Europa sequences. These sequences are much less ΔV efficient than the Callisto-Ganymede-Io sequences and are comparable in ΔV cost to Ganymede-Io double flyby sequences, but they can avoid the radiation to some degree (although not as much as Callisto-Ganymede sequences). The ΔV versus perijove of these sequences are tabulated in Table 10 for perijoves greater than Io's orbital radius.

Table 10. ΔV for Callisto, Ganymede, and Europa Capture Sequences[a], m/s

Flyby Sequences	JOI (9 R_J) ΔV, m/s	JOI (8 R_J) ΔV, m/s	JOI (7 R_J) ΔV, m/s	JOI (6 R_J) ΔV, m/s
CGEJ	360	330	347	359
CGJE	330	321	342	356
CEJG	360	331	346	358
CJEG	336	322	341	354
GEJC	358	326	343	355
GJEC	331	318	337	351
EJGC	358	328	342	354
JEGC	341	319	337	350

[a] V_∞ is 5.6 km/s and flyby altitudes are 300 km.

The remaining types of Callistan triple-satellite-aided capture sequences are Callisto-Europa-Io sequences. However, these sequences are substantially less ΔV efficient than Callisto-Ganymede-Io sequences in ΔV and do not offer the radiation avoidance benefits of Callisto-Ganymede-Europa sequences.

Integrated Triple-Satellite-Aided Capture

We construct triple-satellite-aided capture sequences in STK by adding an extra flyby to double-satellite-aided capture sequences. A double-satellite-aided capture sequence is converged for the first two moons in the three-moon sequence. Then, the trajectory is propagated as usual, and the distance between the spacecraft's nominal trajectory and the third moon is observed. If the third moon is sufficiently close to the nominal

trajectory, the target radius of perijove, the ΔV_{JOI}, or the B-plane parameters of the second flyby can be manually varied to get an optimal three-moon sequence.

Integrated Callistan Triple-Satellite-Aided capture. Callistan triple-satellite-aided capture sequences occur aperiodically, so we search for them by converging double-satellite-aided capture sequences for the first two moons every synodic period (as seen in Table 2) or by using the near-resonance analysis. Once the third moon is sufficiently close to the double-satellite-aided capture trajectory, manually varying the input parameters allows the B-plane of the third moon to be targeted which creates an optimal Callistan satellite-aided capture trajectory.

The near-resonance of the sequences involving Callisto, Io, and Ganymede determines the existence and perijoves of Callisto-Ganymede-Io-JOI and JOI-Io-Ganymede-Callisto sequences over time. Figure 8 shows that JOI-Io-Ganymede-Callisto opportunities tend to decrease in perijove over time until they reach approximately Jupiter's radius and then there is a 1.5 year gap before the next window opens. We call this behavior a "descending staircase" pattern. Similarly, Callisto-Ganymede-Io-JOI sequences follow a similar pattern, except that they tend to increase in perijove over time rather than decrease. We call this behavior an "ascending staircase" pattern.

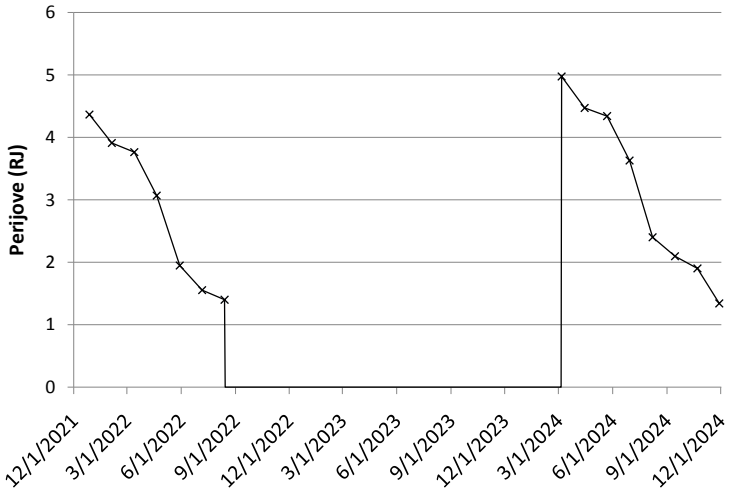

Figure 8 Two flyby windows for JOI-Io-Ganymede-Callisto satellite-aided capture sequences. These sequences follow a "descending staircase" pattern (i.e. a year-long window of JOI-Io-Ganymede-Callisto trajectories exist with perijoves decreasing over time. After that year, no trajectory exists for a two-year gap until another year-long window opens.)

As illustrated in Figure 9, Callisto-Ganymede-JOI-Io sequences occur more frequently than the previous two sequences because there is a JOI maneuver in-between the flybys. There are two opportunities per near-resonance period, and a similar ascending behavior increases the perijoves of the two separate opportunities over time. Additionally, the frequency of Io-JOI-Ganymede-Callisto sequences is also about two opportunities per near-resonance period. Also, the perijoves of each of the two separate opportunities follow a decreasing rather than increasing behavior over time.

We assume without direct integration that the other four Callisto, Ganymede, Io flyby sequences behave

similarly to the first four. The other two sets of Callistan-satellite-aided capture—Callisto, Ganymede, and Europa; and Callisto, Europa, and Io—do not have a convenient near-resonance, so it is likely that they do not exhibit a clear pattern.

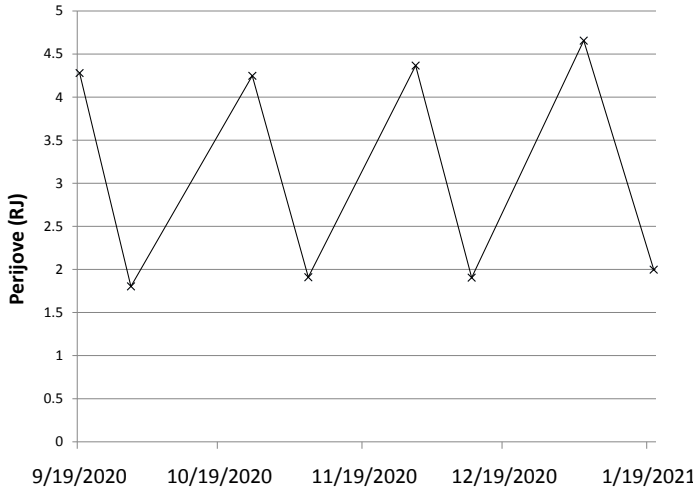

Figure 9 Eight successive flybys that illustrate the general behavior of Callisto-Ganymede-JOI-Io satellite-aided capture sequences. Like the Callisto-Ganymede-Io-JOI sequence, the Callisto-Ganymede-JOI-Io sequence's perijoves trend upward over time. However, there are two available trajectories every 37 days rather than only one, and it appears that a trajectory always exists.

Integrated Laplacian Triple-Satellite-Aided Capture. Laplacian triple-satellite-aided capture sequences involving Io, Europa, and Ganymede only occur once every period of the Laplace resonance (7.0509 days). The previous patched-conic analysis proved that there are only four geometric configurations of the moons that produce optimal satellite-aided capture sequences. Even these four configurations are constrained by a very tight range of perijoves. Hence, the target perijoves must be manually varied in order to obtain sequences that do not require an excessive amount of ΔV to target the final flyby. These three-moon encounters are rarely in the same plane. Thus, the trajectory requires at least one component of the JOI manuever or a suboptimal B-plane angle to target the plane of the post-JOI flybys. If the B-plane angle deviation or the JOI out-of-plane component becomes large, the JOI maneuver becomes suboptimal.

Once we converge a particular Laplacian triple-satellite-aided capture sequence, we can find other sequences by changing the input epoch by about 7 days and allowing the targeter to re-converge. Thoroughly searching through these sequences every 7 days allows Laplacian triple-satellite-aided capture sequences to be found that either perform an extra gravity assist at Callisto, align with an ideal interplanetary trajectory, or both (under rare circumstances).

Triple Flyby Navigation Results

Results from the delta-Delta-v method indicate geometrically increasing flyby errors at each subsequent satellite encounter; thus, navigating triple-satellite-aided capture trajectories poses a difficult challenge. The first flyby causes a significant error in the second flyby, which, in turn, causes an extreme error in the third

flyby. The flyby error results for the Callisto, Io, and Ganymede sequences (which provide the lowest ΔV for triple-satellite-aided captures) are tabulated in Table 12. For example, the first entry in the table, 110 km, corresponds to the Ganymede flyby error that was caused by a 10 km error in the Callisto flyby of a Callisto-Ganymede-Io-JOI sequence with a perijove of 5 R_{J}. The entry directly below, 880 km, corresponds to the error in the Io flyby in the same sequence that was caused by the first two flybys of Callisto and Ganymede. The results for the four existent Laplacian triple-satellite-aided capture sequences are tabulated in Table 11.

Table 11 Flyby Errors due to a 10-km Flyby Error in the First Flyby on the Two Subsequent Flybys[a], km

Sequence	Perijove (R_{J})	Second Flyby	Third Flyby
GEJI	1.15	31	-120
GIJE	2.16	54	-390
EJIG	2.15	84	420
IJEG	1.11	66	210

[a]Laplace resonance cases (Io, Europa, and Ganymede).

Table 12 Flyby Errors due to a 10-km Flyby Error in the First Flyby on the Two Subsequent Flybys[a], km

Perijove	5 R_{J}	4 R_{J}	3 R_{J}	2 R_{J}	1 R_{J}
CGIJ Ganymede flyby	110	100	94	88	82
CGIJ Io flyby	880	690	570	470	380[b]
CGJI Ganymede flyby	110	100	94	88	82
CGJI Io flyby	-1300	-1200	-1000	-880	-700
CIJG Io flyby	180	170	150	140	130
CIJG Ganymede flyby	-3000	-2200	-1700	-1300	-970
CJIG Io flyby	240	250	240	220	200
CJIG Ganymede flyby	2500	1800	1300	1000	740
GIJC Io flyby	82	69	60	53	47
GIJC Callisto flyby	3200	2200	1600	1200	910
GJIC Io flyby	140	150	150	130	110
GJIC Callisto flyby	3800	2900	2300	1700	1200
IJGC Ganymede flyby	300	280	250	220	170
IJGC Callisto flyby	5600	4700	3900	3100	2200
JIGC Ganymede flyby	370	350	300	230	150
JIGC Callisto flyby	4100	3500	2800	2000	1200

[a]Non-resonant cases (i.e involving Callisto).
[b]This is the smallest error at Io; the Ganymede flyby error was 82 km and the Io flyby error was 380 km.

These ballistically propagated results show that a successful implementation of these triple-flyby sequences requires either an extremely accurate nominal trajectory or active autonomous navigation techniques. We note that these errors scale nearly linearly. If the first flyby error could be reduced to 1 km, each of the following flyby errors could be decreased by a factor of approximately one-tenth.

QUADRUPLE-SATELLITE-AIDED CAPTURE

Patched Conic Quadruple-Satellite-Aided Capture

The Laplace resonance constrains quadruple-satellite-aided capture sequences to only occur when Callisto is encountered before or after one of the four physically possible Laplacian triple-satellite-aided capture sequences. Due to the restrictive constraints on Callisto's position, optimal quadruple-satellite-aided capture sequences are rare. However, a patched-conic analysis can still be done to determine the required ΔV for such sequences. An extra Callisto gravity assist just needs to be modeled before or after a complete Laplacian triple-satellite-aided capture sequence. There exist four Laplacian triple-flyby sequences, and a Callisto flyby is allowed before or after each sequence; therefore, eight quadruple-satellite-aided capture sequences exist. The ΔV of these sequences, their required perijoves, and the perijoves of the final orbits are tabulated in Table 13.

Table 13. Quadruple-Satellite-Aided Capture Sequences[a]

Flyby Sequences	JOI ΔV, m/s	Perijove Radius, R_{J}	Final Orbit Perijove Radius, R_{J}
CGIJE	175	2.16	2.08
CEJIG	177	2.11	1.77
GIJEC	175	2.16	1.61
EJIGC	176	2.11	1.34
CGEJI	160	1.15	1.10
CIJEG	161	1.15	0.91
GEJIC	159	1.15	0.79
IJEGC	160	1.15	0.64

[a] V_∞ is 5.6 km/s and flyby altitudes are 300 km.

Integrated Quadruple-Satellite-Aided Capture

As mentioned in the previous section, we find integrated quadruple-satellite-aided capture sequences by searching through all occurrences of each type of Laplacian triple-satellite-aided capture, and observing when these trajectories come within about 30,000 km of Callisto. Once such a trajectory is found, several parameters must be manually modified to allow the trajectory to properly target a reasonably optimal Callisto flyby. Callisto's $B \cdot R$ can be targeted by adding an out-of-plane component to the JOI maneuver or forcing the previous flyby to have a suboptimal B-plane angle. Callisto's $B \cdot T$ can be targeted by manually varying the target radius of perijove and changing the anti-velocity component of the JOI manuever. These variations modify the capture orbit from the standard 200-day orbit used in all the other cases, but are usually necessary to converge a quadruple-satellite-aided capture trajectory.

A sample integrated quadruple-satellite-aided capture trajectory occurs in September of 2022 and is classified as a Ganymede-Io-JOI-Europa-Callisto capture sequence. This trajectory was discovered by converging Ganymede-Io-JOI-Europa capture sequences until Callisto passed within about 30,000 km of the trajectory. The search began by finding Ganymede-Io-JOI-Europa sequences that occur over the arrival window from September 2020 to September 2022. The fact that only one quadruple-satellite-aided capture sequence of either of two particular types (Callisto-Ganymede-Io-JOI-Europa or Ganymede-Io-JOI-Europa-Callisto) was found in a two-year period attests to their infrequency.

The STK trajectory had six significant events: the initial state, the Ganymede flyby, the Io flyby, the JOI maneuver, the Europa flyby, and the Callisto flyby. The initial state is characterized by a hyperbolic six-state and initial time given by Table 14. We characterize the flybys in Table 15 by B-plane parameters, flyby altitude, B-plane angle, and time. The JOI maneuver is characterized by its ΔV and azimuth angle and the capture orbit period in Table 16.

The integrated Ganymede-Io-JOI-Europa-Callisto sequence was 30 m/s more costly than an equivalent patched-conic trajectory. The primary causes of this inefficiency are the out-of-plane errors in the Europa flyby and gravity losses due to the finite-burn JOI maneuver.

Table 14. Integrated GIJEC Flyby Sequence: Initial State

Initial Time (UTC)	Target Rp (R_{J})	V_∞ (km/s)	RA (deg)	Dec. (deg)	$V_{\text{azimuth},p}$	TA (deg)
21 Sept 2022 5:14	2.5045	5.600	344.99	-0.4481	92.3192	209.09

Table 15. Integrated GIJEC Flyby Sequence: Flyby Parameters

Flyby Times (UTC)	Flyby Body	Altitude(km)	Θ (deg)	$B \cdot R$ (km)	$B \cdot T$ (km)
24 Sept 2022 17:13	Ganymede	300.3	0.0	0.0	2972
25 Sept 2022 3:46	Io	255.8	0.0	0.0	2100
25 Sept 2022 16:15	Europa	245.7	134.7	1293	-1281
26 Sept 2022 18:06	Callisto	276.3	180.0	0.0	-2700

Quadruple Flyby Navigation Results

Quadruple-satellite-aided capture sequences are notably less sensitive to flyby errors than many of the triple-satellite-aided capture sequences due to the fact that they only occur at low perijoves. However, quadruple-flyby sequences still require active trajectory corrections between flybys in order to ensure that the final flybys are targeted correctly. Table 17 shows the propagation of errors for all of the quadruple-satellite-aided capture sequences.

DISCUSSION

We emphacize that the integrated trajecories presented here are purely deterministic. Our intent is to demonstrate the physical realizability of multiple-satellite-aided capture. If we had not demonstrated the existence of such trajectories, further analysis would not be indicated. However, due to the significant benefit that these capture trajectories offer, the question of whether they can be made feasible from a navigation and mission operation perspective may be worth further study. In this paper, we have ignored many important issues that must be resolved including the statistical effects of errors in flyby conditions, non-gravitational forces, spacecraft maneuver errors (in particular ΔV_{JOI} magnitude and pointing errors), ephemeris errors, etc. Clearly, those issues are beyond the scope of the present study.

CONCLUSIONS

Several types of multiple-satellite-aided capture trajectories (with two, three, and four satellites) have been computed with a high-fidelity propagation model. A rough $\delta(\Delta V)$ analysis was used to approximate the sensitivities of these trajectories to small flyby errors. Based on this analysis, we conjecture that if the first flyby (of many of these sequences) could be targeted to an accuracy of within 1 km of the nominal trajectory, then the use of such capture sequences may become practical.

The ΔV savings of these multiple-satellite-aided capture over unaided capture range from 210 m/s at about 1 R_{J} to 847 m/s at 14 R_{J}. The triple-satellite-aided capture case includes four unique solutions for Ganymede, Europa, and Io sequences that were derived from the Laplace resonance. In contrast, the non-resonant Callistan satellite-aided capture sequences have a continuum of possible solutions, but most of the sequences occur less frequently than the Laplace-resonant sequences.

It is expected that significant advantages in navigation and spacecraft control will be necessary to realize

Table 16. Integrated GIJEC Flyby Sequence: Jupiter Orbit Insertion

JOI Time (UTC)	Rp (R_{J})	ΔV(m/s)	Orbit Period (days)	JOI duration (s)	JOI az. (deg)
25 Sept 2022 8:05	2.1439	220.3	167.6	1032.41	-160.6

Table 17. Error due to a 10-km Flyby Error in the First Flyby on the Three Subsequent Flybys, km

Sequence	Perijove (R_J)	Second Flyby	Third Flyby	Fourth Flyby
CGEJI	1.15	83	260	-960
CGIJE	2.16	89	480	-2600
CEJIG	2.11	120	-540	-3800
CIJEG	1.15	130	-610	-2100
GEJIC	1.15	31	-140	-1700
GIJEC	2.16	54	-360	-4400
EJIGC	2.11	72	350	3000
IJEGC	1.15	89	190	1600

the significant ΔV (and therefore propellant) savings that multiple-satellite-aided capture promises.

ACKNOWLEDGMENTS

The authors thank Nathan Strange at the Jet Propulsion Laboratory for his helpful suggestions. The first author was supported by Purdue University's Charles C. Chappelle fellowship.

REFERENCES

[1] R. W. Longman, "Gravity Assist from Jupiter's Moons for Jupiter-Orbiting Space Missions," tech. rep., The RAND Corp., Santa Monica, CA, 1968.

[2] R. W. Longman and A. M. Schneider, "Use of Jupiter's Moons for Gravity Assist," *Journal of Spacecraft and Rockets*, Vol. 7, No. 5, May 1970, pp. 570–576.

[3] J. K. Cline, "Satellite Aided Capture," *Celestial Mechanics*, Vol. 19, May 1979, pp. 405–415.

[4] K. T. Nock and C. Uphoff, "Satellite Aided Orbit Capture," *AAS Paper 79-165, Proceedings of the AAS/AIAA Astrodynamics Specialist Conference*, Provincetown, MA, June 25–27, 1979.

[5] M. Malcolm and C. McInnes, "Spacecraft Planetary Capture Using Gravity-Assist Maneuvers," *Journal of Guidance, Control, and Dynamics*, Vol. 28, March-April 2005, pp. 365–368.

[6] C. H. Yam, *Design of Missions to the Outer Planets and Optimization of Low-Thrust, Gravity-Assist Trajectories via Reduced Parameterization*. PhD thesis, School of Aeronautics and Astronautics, Purdue University, West Lafayette, IN, May 2008, pp. 96–104.

[7] M. G. Wilson, C. L. Potts, R. A. Mase, C. A. Halsell, and D. V. Byrnes, "Manuever Design for Galileo Jupiter Approach and Orbital Operations," *Space Flight Dynamics, Proceedings of the 12th International Symposium*, Darmstadt, Germany, June 1997, pp. 1–9.

[8] T. Sweetser, R. Maddock, J. Johannesen, J. Bell, P. Penzo, A. Wolf, S. Williams, S. Matousek, and S. Weinstein, "Trajectory Design for a Europa Orbiter Mission: A Plethora of Astrodynamic Challenges," *AAS Paper 97-174, Proceedings of the AAS/AIAA Space Flight Mechanics Meeting*, Huntsville, AL, February 1997.

[9] J. R. Johannesen and L. A. D'Amario, "Europa Orbiter Mission Trajectory Design," *AAS Paper 99-330, Proceedings of the AAS/AIAA Astrodynamics Conference*, Vol. 103, Girdwood, AK, August 1999.

[10] A. F. Heaton, N. J. Strange, J. M. Longuski, and E. P. Bonfiglio, "Automated Design of the Europa Orbiter Tour," *Journal of Spacecraft and Rockets*, Vol. 39, No. 1, January-February 2002, pp. 17–22.

[11] G. J. Whiffen and T. Lam, "The Jupiter Icy Moons Orbiter reference trajectory," *AAS Paper 06-186, Proceedings of the AAS/AIAA Space Flight Mechanics Meeting*, Tampa, FL, January 2006.

[12] P. S. Laplace, *The System of the World*. Old Bailey, London, UK: W. Flint, 1809. Translated by J. Pond.

[13] A. T. Sinclair, "The Orbital Resonance Amongst the Galilean Satellites of Jupiter," *Celestial Mechanics*, Vol. 12, 1975, pp. 89–96.

[14] A. P. Showman and R. Malhotra, "Tidal Evolution into the Laplace Resonance and the Resurfacing of Ganymede," *Icarus*, Vol. 127, 1997, pp. 93–111.

[15] S. Musotto, F. Varadi, W. Moore, and G. Schubert, "Numerical Simulations of the Orbits of the Galilean Satellites," *Icarus*, Vol. 159, 2002, pp. 500–504.

[16] "Analytical Graphics, Inc. STK/Astrogator background information," http://www.stk.com/resources/download/astrogator/astrogator_resources.cfm.

[17] B. Buffington, N. Strange, and R. Ionasescu, "Addition of a Low Altitude Tethys Flyby to the Nominal Cassini Tour," *AAS Paper 05-270, Proceedings of the AAS/AIAA Astrodynamics Specialists Conference*, Reno, NV, August 2005.

[18] R. A. Broucke, "The Celestial Mechanics of Gravity Assist," *AIAA Paper No. 88-4220-CP, Proceedings of the AIAA/AAS Astrodynamics Specialist Conference*, Minneapolis, MN, August 1988, pp. 69–78.

[19] J. D. Anderson, E. L. Lau, W. L. Sjogren, G. Schubert, and W. B. Moore, "Gravitational Constraints on the Internal Structure of Ganymede," *Nature*, No. 384, December 1996, pp. 541–543.

[20] J. D. Anderson, R. A. Jacobson, T. P. McElrath, W. B. Moore, G. Schubert, and P. C. Thomas, "Shape, Mean Radius, Gravity Field, and Interior Structure of Callisto," *Icarus*, No. 153, 2001.

[21] J. D. Anderson, R. A. Jacobson, E. L. Lau, W. B. Moore, and G. Schubert, "Io's Gravity Field and interior Structure," *Journal of Geophysical Research*, No. 106, 2001.

[22] J. D. Anderson, G. Schubert, R. A. Jacobson, E. L. Lau, W. B. Moore, and W. L. Sjogren, "Europa's Differentiated Internal Structure: Inferences from Four Galileo Encounters," *Science*, No. 281, 1998.

[23] K. B. Clark, T. Magner, R. Pappalardo, M. Blanc, R. Greeley, J. P. Lebreton, C. Jones, and J. C. Sommerer, "Jupiter Europa Orbiter Mission Study 2008: Final Report," tech. rep., Task Order No.: NMO710851, JPL, Pasadena, CA, 2009.